Indonesian Journal of Environmental Management and Sustainability
e-ISSN:2598-6279 *p*-ISSN:2598-6260

IJEMS

Research Paper

Utilization of Hydroxyapatite from Quail Eggshells as an Adsorbent for Lead Metal Ions Pb(II)

Matlal Fajri Alif[1*], Syukri Darajat[1], Siti Azizah[1]

[1] *Department of Chemistry, Faculty of Mathematics and Natural Sciences, Andalas University, Padang, 25163, Indonesia*
***Corresponding author e-mail**: mfalif@sci.unand.ac.id

Abstract
Lead is a toxic metal known for its harmful effects, even in minor quantities, because it does not break down naturally and can therefore pollute ecosystems. This research involved the creation of hydroxyapatite using quail egg shell through a sol-gel method, which served as a medium for capturing Pb ions in a batch process by assessing different parameters. The created material was analyzed using X-Ray Diffraction (XRD) to confirm its crystal form, SEM (Scanning Electron Microscopy) to analyze its surface, FTIR (Fourier Transform Infrared Spectroscopy), and morphology to determine the functional units that were present. Sorption tests were performed under various scenarios, encompassing different pH levels, the initial Pb ion concentration, and time of contact, with the outcome evaluated through atomic absorption spectrophotometry (AAS). The results demonstrated that the optimal conditions for Pb ion uptake were observed at a concentration of 800 mg/L with 0.1 g of absorbent as well as a contact time of 60 minutes, achieving a lead ion removal rate of 71.48%. The sorption isotherm followed the Langmuir model, while the sorption kinetics fit the pseudo-order two model, indicating a monolayer sorption mechanism on a uniform surface. These outcomes suggest hydroxyapatite derived from quail eggshells is a promising eco-friendly material for treating wastewater containing heavy metal ions.

Keywords
Hydroxyapatite, Adsorption, Quail Eggshell, Lead Metal Pb(II)

Received: 10 December 2024, Accepted: 26 February 2025
https://doi.org/10.26554/ijems.2025.9.1.20-27

1. INTRODUCTION

Among the various contaminants often found in water, industrial effluents, heavy metals, and dyes play a significant role. These substances generally come from industrial activities such as mining, metal plating and smelting, the textile and dye industry, leather tanning, pesticide production and fermenters, papermaking, and the paint industry. Indiscriminate disposal of heavy metals and dyes beyond the prescribed limits can have serious impacts on health and become a major cause of environmental problems (Amenaghawon et al., 2022). Toxic heavy metals like lead (Pb) are commonly present in water environments. As per the regulations established by the WHO (World Health Organization), the limited allowable concentration of lead (Pb) in water is 0.05 mg/L. Research shows that lead (Pb) exposure can cause brain disorders, cancer, anorexia, anemia, kidney damage, and dementia (Li et al., 2024). Multiple methods have been utilized to address these issues, as example flocculation, chemical precipitation, neutralization, ion exchange, adsorption, and membrane separation. Nevertheless, numerous approaches encounter challenges like expensive equipment, complications in execution, generation of harmful sludge, and significant operational expenses. On the contrary, adsorption stands out as a cost-effective, the most straightforward, eco-friendly, easy-to-execute, as well as efficient solution (Kotnala et al., 2024).

Commonly utilized materials for extracting heavy metals consist of activated carbon, zeolites, chitosan, ion exchange resins, industrial solid waste, and hydroxyapatite (Yan et al., 2014). The implementation of hydroxyapatite in the extraction of heavy metals has garnered significant attention from researchers, mainly due to its plentiful availability, eco-friendly characteristics, and ion exchange capabilities. The presence of calcium ions (Ca^{2+}), phosphate ions (PO_4^{3-}), and hydroxyl ions (OH^-) ions makes HAp have both positive and negative surface charges, making it capable of bonding with various other atoms (Xu et al., 2023). Hydroxyapatite can be synthesized using calcium-based materials from natural materials such as limestone shells, eggshells, and green mussel shells (Alif et al., 2024). The potential for eggshell waste in Indonesia is quite large. One of them is

quail eggshell, which makes up approximately 10% of the egg's total weight and is often a waste from the egg processing industry and households, although it is sometimes used in small-scale applications. The primary elements of quail eggshell are calcium carbonate (over 95%) and protein, a viable alternative to calcium carbonate that can be efficiently obtained and utilized in the process of making hydroxyapatite (Vinayagam et al., 2023). The utilization of quail eggshells as a source of calcium in hydroxyapatite synthesis is an environmentally friendly process because it utilizes waste to prevent environmental pollution. The purpose of this investigation is to analyze the efficacy of hydroxyapatite derived from quail eggshells in absorbing lead metal ions (Pb), utilizing various factors assessed through XRD, SEM, and FTIR methods.

2. EXPERIMENTAL SECTION

2.1 Materials and Instruments

Quail eggshells were collected from Lima Puluh Kota District, West Sumatra, Indonesia. Diammonium phosphate ($(NH_4)_2HPO_4$), nitric acid (HNO_3), potassium nitrate (KNO_3), potassium hydroxide (NaOH), and $Pb(NO_3)$ all produced by Merck, were used in this study. All analytical reagents were dissolved using distilled water (H_2O). The equipment used in this study consisted of mortar and pestle, thermo insight (furnace), analytical balance, hot plate, oven (Labtech), pH meter, magnetic stirrer, 200 mesh sieve (75 μm), burette, rotary shaker (Edmun Buhler 7400 Tubingen), and necessary laboratory glassware. Analysis and characterization of the adsorbents were performed by AAS (Shimadzu AA7000G, Autosampler), SEM-EDX (Carl Zeiss Scanning Electron Microscope With EDX EVO 10) and FTIR (PerkinElmer version 10.6.1).

2.2 Methods

2.2.1 Sample Preparation

The collected quail eggshells were washed using running water, then the shells were boiled for 30 minutes at 100°C to remove impurities and rinsed using distilled water. Next, the quail eggshells were oven-dried at 105°C for half an hour. The dried quail eggshells were reduced in size until they became powder. Furthermore, quail eggshell powder was sieved using a 200 mesh sieve (75 μm) which aims for size uniformity. Quail eggshell powder was calcined for 5 hours at 900°C using a furnace (Alif et al., 2018). The quail eggshell powder was then used in the hydroxyapatite synthesis process.

2.2.2 pHpzc (Point Zero Charge) Study

Adsorption experiments and point zero charges were performed by combining the adsorbent (0.1 g) with 0.1 M KNO_3 (50 mL) across various pH levels. The concluding pH was assessed, and a graph was generated contrasting it with the starting pH. The intersection point of the curve that cuts through the zero marker on the X-axis represents the point of zero charge or pHpzc (zero charge point). The variation in pH (ΔpH) at equilibrium was determined by applying the formula ΔpH = (pHf - pHi) (Hassan et al., 2020).

2.2.3 Adsorption Study

A total of 0.1 g of hydroxyapatite adsorbent was put into 50 mL of Pb(II) metal ion solution with solution pH 4. Then the concentration of the solution was adjusted with a concentration variation of 100 - 1000 mg/L. Then dishaker for 60 minutes at a speed of 200 rpm. After obtaining optimum absorption conditions at certain concentrations, experiments were then carried out to identify the ideal choice mass and contact time for the absorption of Pb(II) metal ions by hydroxyapatite. The mixture was subsequently strained, and the filtrate was measured by AAS (Putra et al., 2024). The sorption capability of Pb(II) metal ions was decided by applying Equation 1:

$$q = \frac{C_0 - C_e}{m} \times V \tag{1}$$

The proportion absorption of Pb(II) metal ions can be determined in Equation 2:

$$R = \frac{C_0 - C_e}{C_0} \times 100\% \tag{2}$$

The sorption capacity (qe) of Pb(II) metal ions retained by the hydroxyapatite adsorbent (measured in mg/g) is determined using the primary (Co) as well as last (Ce) concentrations of metal ions in the solution (mg/L), the solution volume (V) in liters, and the mass (g) of the adsorbent used in grams.

3. RESULTS AND DISCUSSION

3.1 pHpzc and Adsorption Studies

The pH point of zero charge, or pHpzc, plays an essential part in shaping the surface charge of an adsorbent. At this specific pH level, the total charge on the adsorbent becomes neutral, which occurs under specified conditions of temperature, pressure, and solution makeup. The pHpzc signifies that, at this pH, the total count of positive surface charges matches the total count of negative charges. Establishing the pHpzc has an impact on the adsorption percentage, which varies depending on the material in question (Al-Maliky et al., 2021). pHpzc of hydroxyapatite adsorbent is fully visible in Figure 1.

According to Figure 1, the determination of pHpzc is done by determining the intersection point between The initial pH curve as well as the last pH curve of the solution. Determination of pHpzc causes changes in the speciation of target adsorbate molecules, where if the pH of the target solution >pHpzc indicates that the adsorbent surface holds a full positive charge as a result of protonation, but if the pH of the target solution <pHpzc indicates that the adsorbent surface is negatively charged due to deprotonation

© 2025 The Authors.

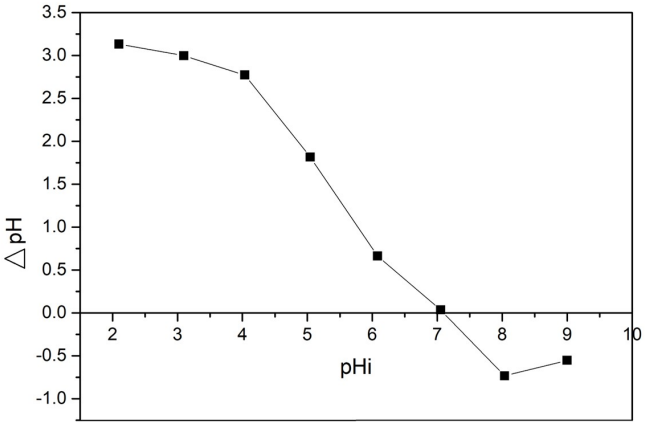

Figure 1. pHpzc Hydroxyapatite

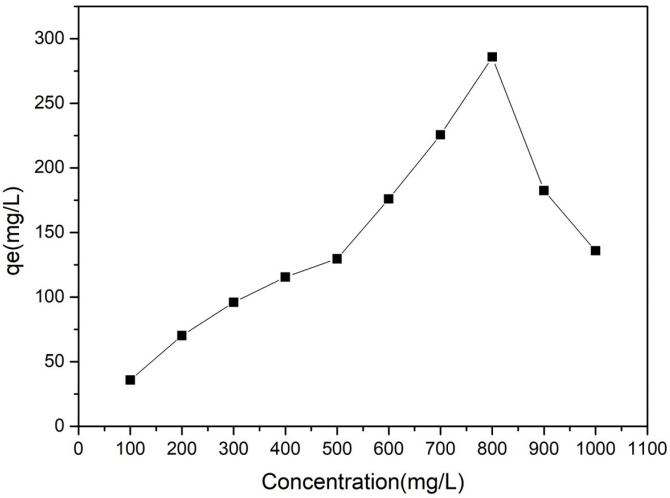

Figure 2. Impact of Initial Levels of Heavy Metals on the Adsorption Ability of Hydroxyapatite, Ideal pH (pH 4), Contact Duration 60 Minutes, Agitation Frequency 200 rpm, and Adsorbent Weight 0.1 g

(Adawiyah et al., 2024). Hydroxyapatite has a neutral charge at pH 7.05 When the pH is less than phPzc, it causes hydroxyapatite to be positively charged so that it can be used in anionic absorption and vice versa (Zein et al., 2024). According to the evaluation of pHpzc, the impact of pH on the absorption of Pb(II) metal ions is carried out in the range of 3 - 8 obtaining optimal conditions at pH 4.

3.2 Effect of Concentration and Isotherm Evaluation

The goal of concentration assessment is to evaluate how the quantity of active sites present on the adsorbent's surface relates to the rise in solution concentration. The influence of solution concentration on the ability to absorb Pb(II) metal ions with hydroxyapatite as the adsorbent is illustrated in Figure 2.

Figure 2, shows that the concentration increases as the adsorbate concentration increases. The rise in the capacity for metal ion adsorption is attributed to multiple elements including the relationship between metallic surfaces and metal ions, the ability to diffuse, and the existence of functional sites on the surface of the adsorbent (Bilal et al., 2024). This phenomenon is evident as the concentration of the adsorbate rises from 100 mg/L to 800 mg/L, attributed to the active sites of hydroxyapatite that are capable of interacting with Pb(II) metal ions. The peak absorption concentration for Pb(II) metal ions was attained at 800 mg/L, showcasing an absorption capability of 285.93 mg/g as well as an absorption efficiency of 71.48 for Pb(II) metal ions. The optimal concentration indicates that there has been an equilibrium between the concentration of Pb(II) metal ions that have been absorbed with the hydroxyapatite adsorbent (Wang et al., 2018). After reaching the optimal concentration, the adsorption capability decreased at a concentration of 900 mg/L - 1000 mg/L because hydroxyapatite had reached the saturation point. The adsorption isotherm model aims to determine the interaction between Pb(II) metal ions in liquid and solid phases when reaching equilibrium to obtain the right correlation (Li et al., 2024). Langmuir Model can be determined Equation 3:

$$\frac{1}{q_e} = \frac{1}{k_l q_m C_e} + \frac{1}{q_m} \tag{3}$$

where qe is the adsorption capacity (mg/g), ce is the concentration (mg/L) at equilibrium, qm is the maximum monolayer adsorption capacity (mg/g) and KL is the Langmuir constant (L/mg). Freundelich Model can be determined by Equation 4:

$$\log q_e = \log K_f + \frac{1}{n} \log C_e \tag{4}$$

where Kf is the Freundilch constant (L/mg), and n is the adsorption strength. The adsorption isotherm model achieves balance by satisfying the Langmuir isotherm equation, exhibiting a maximum absorption capability of 285.93 mg/g. This suggests that the adsorption happens on a uniform surface containing similar binding sites, generating the creation of a single layer on the adsorbent's surface, known as monolayer adsorption (Zeng et al., 2018). The results from the curve indicate that the Langmuir isotherm model produced a linear equation represented by y = 0.0094x + 0.0251, illustrating the concept of the coefficient of determination (R^2) of 0.9445, which is near 1, along with a Langmuir constant (K_L) of 0.0539, as shown in Table 1. The Langmuir constant value (K_L) shows the attraction between the adsorbent and heavy metals, where the greater the equilibrium constant value, the greater the affinity of the adsorbent to metals (Trakoolwannachai et al., 2019). Table 1. Freundlich for the adsorption of Pb(II) as well as Parameters from Langmuir ions using hydroxyapatite.

© 2025 The Authors.

Table 1. Langmuir and Freundlich Parameters Regarding the Sorption of Pb(II) Ions Utilizing Hydroxyapatite

Parameters	Langmuir				Freundlich		
Pb(II)	q_{max} (mg/g)	K_L (L/mg)	R_L	R^2	K_F (L/mg)	$1/n$	R^2
	273.9726	0.0539	0.0235	0.9228	97.6517	0.4913	0.619

3.3 Effect of Contact Time and Kinetics Study

The purpose of establishing contact time is to gather data regarding the shortest duration needed by hydroxyapatite to absorb Pb(II) metal ions. Based on collision theory, the reaction rate is influenced by the number of collisions in a unit of time. The more frequent collisions occur, the faster the reaction takes place until it reaches equilibrium conditions (Jaihan et al., 2022). Figure 3 highlights the significance of contact duration on the capacity to absorb Pb(II) metal ions.

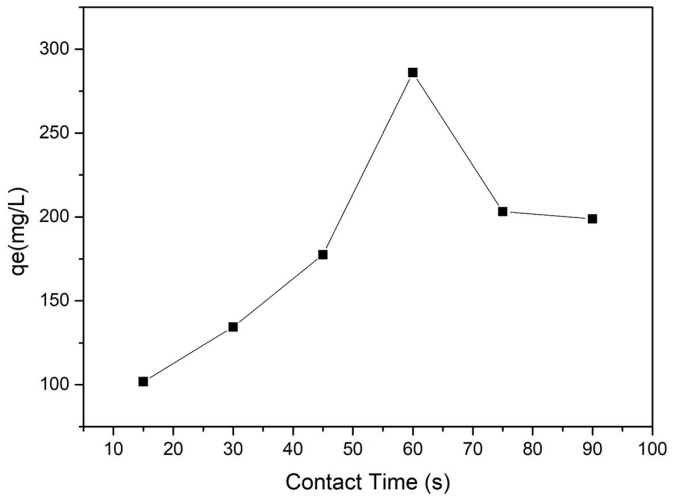

Figure 3. Impact of Initial Metal Weight Concentration on the Adsorption Capability of Hydroxyapatite; Ideal pH (pH 4), Concentration Set at 800 mg/L, Adsorbent Weight 0.1 g, and Agitation Frequency of 200 rpm

Figure 3 illustrates the rise in adsorption capacity from 15 minutes to 60 minutes of contact time. This is because the duration of the collision is extended between hydroxyapatite adsorbent and Pb(II) metal ions, the more Pb(II) metal ions are absorbed by hydroxyapatite adsorbent due to the more active groups on hydroxyapatite adsorbent that bind with Pb(II) metal ions (Wibiyan et al., 2024). The best duration for soaking to absorb Pb(II) metal ions was found to be 60 minutes, achieving an absorption rate of 285.93 mg/g and a metal uptake efficiency for Pb(II) ions at 71.48%. After reaching equilibrium, the ability to adsorb declined due to the surface of the hydroxyapatite adsorbent was closed which caused the obstruction of Pb(II) lead ions to enter the openings of the hydroxyapatite adsorbent (Ali et al., 2016). The reaction kinetics are related to the functional groups

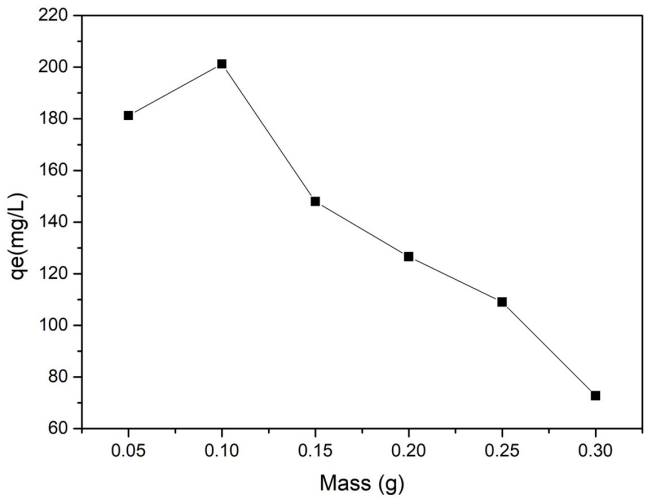

Figure 4. Influence of Adsorbent Weight on the Adsorption Ability for Pb(II) Metal; Ideal pH (pH 4), Concentration 800 mg/L, Contact Duration 60 Minutes, and Stirring Frequency of 200 rpm

and the concentration of adsorbate concentration (Putri et al., 2024). The pseudo-first-order model, the pseudo-second-order model, and the model of intraparticle diffusion sequence were employed to establish the mechanisms of adsorption and the kinetic constants involved in the elimination of heavy metals. The primary pseudo-kinetic model presumes the quantity of pores occupied by the solute is proportional to the adsorption rate (Zhou et al., 2023). The transformed version of the first-order pseudo-kinetic model presented can be determined in Equation 5:

$$\log(q_e - q_t) = \log q_e - \frac{k_1 t}{2.303} \tag{5}$$

where k_1 is the first-order reaction order rate constant, t is time (minutes), qe is the adsorption >capacity (mg/L) at equilibrium, and qt is the amount adopted at a given time. While the second-order model can be determined in Equation 6:

$$\frac{t}{q_t} + \frac{1}{k_2 q_e^2} + \frac{t}{q_e} \tag{6}$$

k_2 manifests the constant of the second order, qe is the adsorption capability (mg/L) at equilibrium, and qt is the amount adopted at a given time. The adsorption kinetics model that occurs between hydroxyapatite and Pb(II)

© 2025 The Authors.

metal ions tends to follow the second-order pseudo adsorption kinetics model (Table 2) which indicates that the reaction system that happens in the adsorption process occurs chemically. It is observable from the curve results that the second-order pseudo adsorption kinetics model obtained a linear equation 0.0037x + 0.0838 with a coefficient of determination R^2 0.8221. The adsorption kinetics model tends to occur when the R^2 value is greater than the other adsorption kinetics models.

3.4 Effect of Adsorbent Mass

The objective of measuring mass is to enhance the ability of hydroxyapatite to adsorb Pb(II) metal ions during the absorption process. The influence of the mass of the hydroxyapatite adsorbent on its capacity to absorb Pb(II) ions is illustrated in Figure 4.

As displayed in Figure 4 the capacity for adsorption rises as the mass increases from 0.05 grams to 0.1 grams. This is due to the higher amount of adsorbent leading to an increased quantity of active sites available on the adsorbent's surface (Iconaru et al., 2018). The optimal mass of Pb(II) metal ion absorption was obtained at a mass of 0.1 gram capable of absorbing 285.93 mg/g and Pb(II) metal ion absorption efficiency of 71.48%. The optimal mass indicates that Pb(II) metal ions have been maximally absorbed by hydroxyapatite. After reaching the optimal mass there is a decrease in adsorption capacity from a mass of 0.15 grams - 0.3 grams. The reduction in absorption capability is caused by the solution of Pb(II) metal ions having reached the saturation point to bind with hydroxyapatite (Ramadhani et al., 2020). The more active sides that are not saturated during the adsorption process indicate that more active sides are available to bind between the adsorbent and the metal. The more adsorbent used, it will form coagulation which causes a decrease in the adsorbent's surface area in the process of metal ion absorption (Chaidir et al., 2015).

3.5 Adsorbent Characterization

Hydroxyapatite was analyzed through XRD (X-Ray Diffraction), FTIR (Fourier Transform Infrared), and SEM (Scanning Electron Microscopy) to provide information on the macromolecular structure as well as the chemical makeup of the adsorbent. Analysis using XRD aims to identify the crystal phase in hydroxyapatite. The results of the analysis in the form of a diffractogram that relates the 2θ angle to the peak intensity will then be compared with JCPDS Number 09-0432 data. The diffractogram of hydroxyapatite at 900°C (Figure 5) shows high intensity with most peaks reflecting the hydroxyapatite phase, namely at angles 2θ = 16.63°, 25.79°, 31.51°, 31.89°, 32.66°, and 33.99°. In addition, there are some low-intensity peaks at 2θ = 18.54°, 21.61,° 39.81°, and 42.10°.

Analysis using FT-IR seeks to recognize functional groups in the form of absorption peaks contained in hydroxyapatite. Analysis using FT-IR helps determine the presence of apatite compounds defined by the existence of characteristic groups PO_4^{3-}. The spectrum of hydroxyapatite after and before absorption of Pb(II) metal ions is visible in Figure 6.

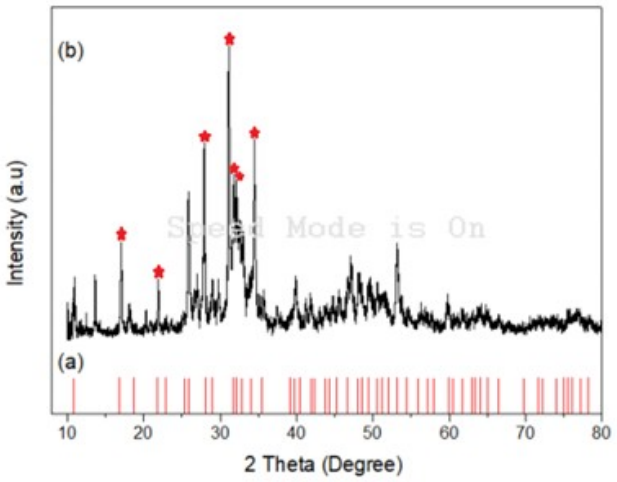

Figure 5. Diffractogram of (a) HAp Standard (JCPDS Number 09-0432) and (b) Hydroxyapatite

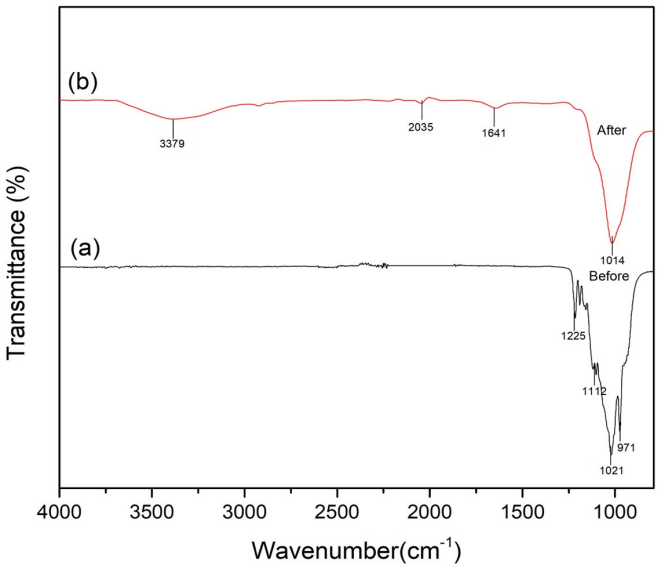

Figure 6. Spectra of Hydroxyapatite (a) Before and (b)>After Pb(II) Metal Ion Absorption.

As shown in Figure 6, it is evident that there is a distinct alteration in the peaks before and after the uptake of Pb(II) ions, suggesting that functional groups like −OH, PO_4^{3-}, and CO_3^{2-} contribute to the adsorption mechanism (dos Santos Horta et al., 2020). The peak observed between 960 and 1100 cm^{-1} relates to the asymmetric stretching vibrations of PO_4^{3-} while the peak around 1225 cm^{-1} is also linked to these asymmetric stretching vibrations. Following

© 2025 The Authors.

Table 2. Pseudo First Order and Pseudo Second Order Parameters for the Absorption of Pb(II) Metal Ions Using Hydroxyapatite

Parameters	Pseudo First Order			Pseudo Second Order		
Pb(II)	K_1 (min^{-1})	q_e (mg/g)	R^2	K_2 (min^{-1})	q_e (mg/g)	R^2
	-0.033	147.142	0.077	0.0050	1.0865	0.8221

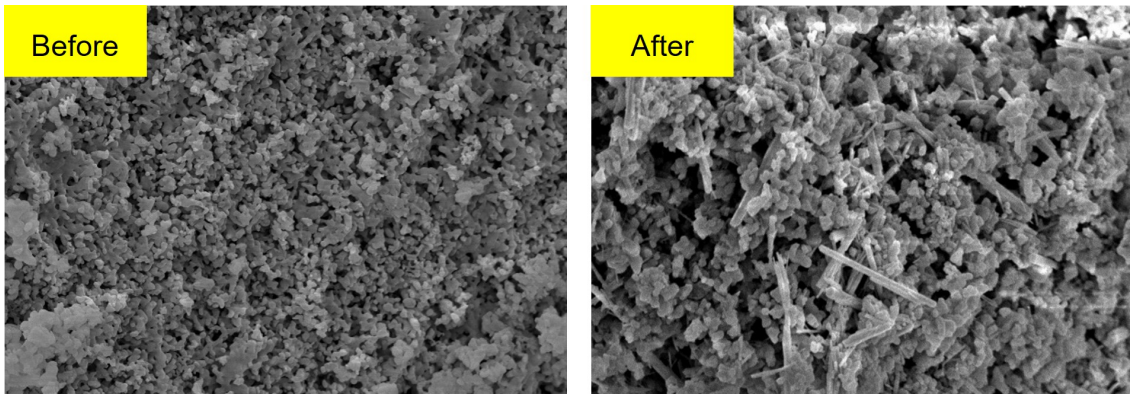

Figure 7. Morphology of Hydroxyapatite Before and After Absorption

the adsorption the peak at 1641 cm^{-1} corresponds to the bending vibrations of H−O−H in bound water (H_2O), along with the way something looks the CO_3^{2-} peak at 2035 cm^{-1} and the O−H peak present at 3379 cm^{-1}. The surface characteristics of hydroxyapatite were analyzed using SEM-EDX under a magnification of 5000x. Figure 7 illustrates the morphological changes occurring after as well as the before adsorption of Pb(II).

Figure 7 reveals the SEM results of hydroxyapatite before and after absorption. Before absorption, the morphology of hydroxyapatite is agglomerated or clumped. Agglomeration is formed when small particles combine at high temperatures to form larger structures produced during the calcination process which causes the particles to coalesce and form agglomerates (Iconaru et al., 2018). After the absorption of Pb(II) metal ions, there is a morphological change in hydroxyapatite, with the appearance of a large number of rod-shaped crystals indicating that Pb(II) metal ions were successfully absorbed by hydroxyapatite. EDX analysis aims to determine the elemental content and qualitative analysis of the Ca/P ratio in hydroxyapatite after as well as before absorption of Pb(II) metal ions. The molar ratio obtained from hydroxyapatite was 1.72 (Table 3).

Table 3. Ca/P Ratio of Hydroxyapatite

Elements	Mass (%)	Ratio
Ca	31.36	1.72
P	18.23	

4. CONCLUSIONS

According to the findings, the levels of concentration, the mass of the adsorbent, and the duration of contact greatly affect the adsorption mechanism of Pb(II) ions when utilizing hydroxyapatite derived from quail eggshells. The best conditions for absorption were established at a concentration of 800 mg/L, an adsorbent weight of 0.1 grams, as well as a contact period of 60 minutes, achieving an absorption efficiency of Pb(II) ions at 71.48%, which corresponds with the Langmuir model and follows pseudo-second-order kinetics.

5. ACKNOWLEDGEMENT

This research was funded by: The Directorate General of Higher Education, Research and Technology, Directorate of Research, Technology and Community Service, Ministry of Education, Culture, Research and Technology, on the Master's Thesis Research Scheme. Following the terms of Research Contract Number: 041/E5/PG.02.00.PL/2024 Fiscal Year 2024.

REFERENCES

Adawiyah, R., N. Yuliasari, Y. Hanifah, K. Alawiyah, and N. R. Palapa (2024). Utilizing *Areca catechu* L. Fruit Peel-Derived Biochar and Hydrochar forCongo Red Adsorption: Kinetic and Thermodynamic Analysis. *Indonesian Journal of Environmental Management and Sustainability*, **8**(4); 135–144

Al-Maliky, E. A., H. A. Gzar, and M. G. Al-Azawy (2021). Determination of Point of Zero Charge (PZC) of Concrete Particle Adsorbents. *IOP Conference Series: Materials Science and Engineering*, **1184**(1); 012004

© 2025 The Authors.

Ali, R. M., H. A. Hamad, M. M. Hussein, and G. F. Malash (2016). The Potential of Using Green Adsorbent of Heavy Metal Removal from Aqueous Solutions: Adsorption Kinetics, Isotherm, Thermodynamic, Mechanism, and Economic Analysis. *Ecological Engineering*, **91**; 317–332

Alif, M. F., W. Aprillia, and S. Arief (2018). Peat Water Purification by Hydroxyapatite (HAp) Synthesized from Waste Pensi (Corbicula Moltkiana) Shells. *IOP Conference Series: Materials Science and Engineering*, **299**(1); 012002

Alif, M. F., R. A. Fitria, S. Arief, S. Triandini, M. Manawan, P. Purnama, and R. Goei (2024). Peat Water Purification Using Nanohydroxyapatite Synthesized from Carbon Negative Precipitated Calcium Carbonate Precursor. *Sustainable Chemistry for the Environment*, **6**(December 2023); 100105

Amenaghawon, A. N., C. L. Anyalewechi, H. Darmokoesoemo, and H. Septya (2022). Hydroxyapatite-Based Adsorbents: Applications in Sequestering Heavy Metals and Dyes. *Journal of Environmental Management*, **302**; 113989

Bilal, M., J. Ali, M. Umar, S. B. Khan, A. Shaheen, N. Hussain, R. Jahan, K. Malook, M. Qayum, K. Akhtar, and E. M. Bakhsh (2024). Ecofriendly Synthesis of Hydroxyapatite from Fish Scales and Its Application Toward Adsorptive Removal of Pb(II). *Journal of the Indian Chemical Society*, **101**(8); 101175

Chaidir, Z., R. Zein, Q. Hasanah, H. Nurdin, and H. Aziz (2015). Absorption of Cr (III) and Cr (VI) Metals in Aqueous Solution Using Mangosteen Rind (Pithecellobium Jirga (Jack) Prain). *J. Chem. Pharm. Res.*, **7**(8); 948–956

dos Santos Horta, M. K., F. J. Moura, M. S. Aguilar, C. B. Westin, J. B. de Campos, S. B. Peripolli, V. S. Ramos, M. I. Navarro, and B. S. Archanjo (2020). Nanostructured Hydroxyapatite from Hen's Eggshells Using Sucrose as a Template. *Materials Research*, **23**(6); 1–9

Hassan, A. F., G. A. El-Naggar, A. G. Braish, M. F. Amira, and L. M. Alshandoudi (2020). Enhanced Adsorption of Chromium(VI) from Aqueous Medium by Basic Nanohydroxyapatite/Chitosan Composite Based on Eggshell. *Desalination and Water Treatment*, **206**; 235–249

Iconaru, S. L., M. Motelica-Heino, R. Guegan, M. Beuran, A. Costescu, and D. Predoi (2018). Adsorption of Pb (II) Ions onto Hydroxyapatite Nanopowders in Aqueous Solutions. *Materials*, **11**(11)

Jaihan, W., V. Mohdee, S. Sanongraj, U. Pancharoen, and K. Nootong (2022). Biosorption of Lead (II) from Aqueous Solution Using Cellulose-Based Bio-Adsorbents Prepared from Unripe Papaya (Carica Papaya) Peel Waste: Removal Efficiency, Thermodynamics, Kinetics and Isotherm Analysis. *Arabian Journal of Chemistry*, **15**(7); 103883

Kotnala, S., B. Bhushan, and A. Nayak (2024). Hydroxyapatite@Cellulose@nZVI Composite: Fabrication and Adsorptive Removal of Doxycycline, Cr(VI) and As(III) from Wastewater. *Chemical Engineering Science*, **288**(October 2023); 119796

Li, X., Y. Cui, W. Du, W. Cui, L. Huo, and H. Liu (2024). Adsorption Kinetics and Mechanism of Pb(II) and Cd(II) Adsorption in Water Through Oxidized Multiwalled Carbon Nanotubes. *Applied Sciences (Switzerland)*, **14**(5)

Putra, A., S. Fauzia, D. Deswati, S. Arief, and R. Zein (2024). The Potential of Duck Egg White as a Modifier for Activated Rice Straw to Enhance Cr(VI) Ions Adsorption in an Aqueous Solution. *South African Journal of Chemical Engineering*, **48**(February 2023); 204–213

Putri, B. I., F. S. Arsyad, and A. Lesbani (2024). Hydrothermal Carbonization of *Eucheuma cottonii* for Selective Adsorption of Anionic Dyes. *Indonesian Journal of Environmental Management and Sustainability*, **8**(4); 154–165

Ramadhani, P., Z. Chaidir, T. Zilfa, Z. B. Tomi, D. Rahmiarti, and R. Zein (2020). Shrimp Shell (Metapenaeus Monoceros) Waste as a Low-Cost Adsorbent for Metal Yellow Dye Removal in an Aqueous Solution. *Desalination and Water Treatment*, **197**; 413–423

Trakoolwannachai, V., P. Kheolamai, and S. Ummartyotin (2019). Characterization of Hydroxyapatite from Eggshell Waste and Polycaprolactone (PCL) Composite for Scaffold Material. *Composites Part B: Engineering*, **173**; 106974

Vinayagam, R., S. Kandati, G. Murugesan, L. C. Goveas, A. Baliga, S. Pai, T. Varadavenkatesan, K. Kaviyarasu, and R. Selvaraj (2023). Bioinspiration Synthesis of Hydroxyapatite Nanoparticles Using Eggshells as a Calcium Source: Evaluation of Congo Red Dye Adsorption Potential. *Journal of Materials Research and Technology*, **22**; 169–180

Wang, Y. Y., Y. X. Liu, H. H. Lu, R. Q. Yang, and S. M. Yang (2018). Competitive Adsorption of Pb(II), Cu(II), and Zn(II) Ions onto Hydroxyapatite-Biochar Nanocomposite in Aqueous Solutions. *Journal of Solid State Chemistry*, **261**; 53–61

Wibiyan, S., I. Royani, N. Ahmad, and A. Lesbani (2024). Assessing the Efficiency, Selectivity, and Reusability of ZnAl-Layered Double Hydroxide and Eucheuma Cottonii Composite in Removing Anionic Dyes from Wastewater. *Inorganic Chemistry Communications*, **170**; 113347

Xu, Y., H. Tang, P. Wu, M. Chen, Z. Shang, J. Wu, and N. Zhu (2023). Manganese-Doped Hydroxyapatite as an Effective Adsorbent for the Removal of Pb (II) and Cd (II). *Chemosphere*, **321**; 138123

Yan, Y., X. Dong, X. Sun, X. Sun, J. Li, J. Shen, W. Han, X. Liu, and L. Wang (2014). Conversion of Waste FGD Gypsum into Hydroxyapatite for Removal of Pb^{2+} and Cd^{2+} from Wastewater. *Journal of Colloid and Interface Science*, **429**; 68–76

Zein, R., D. Deswati, S. Fauzia, and N. F. Pisya (2024). Comparative Study of Pb(II) and Cr(VI) Removal Using *Cassava peel* (Manihot Esculenta Crantz). *International Journal of Phytoremediation*, **26**(13); 2074–2083

Zeng, R., W. Tang, X. Liu, C. Ding, and D. Gong (2018).

© 2025 The Authors.

Adsorption of Cu2+ from Aqueous Solutions by Si-Substituted Carbonate Hydroxyapatite Prepared from Egg-Shell: Kinetics, Isotherms and Mechanism Studies. *Desalination and Water Treatment*, **116**; 137–147

Zhou, C., Q. Zhou, Y. Yu, and S. Ge (2023). Spongy Magnetic Hydroxyapatite for the Enhanced Pb2+ Removal and Its Dynamic Sorption Mechanism. *Journal of Environmental Chemical Engineering*, **11**(4); 110213

© 2025 The Authors.